HHS Public Access

Author manuscript

Circ Res. Author manuscript; available in PMC 2022 January 22.

Published in final edited form as:

Circ Res. 2021 January 22; 128(2): 172–184. doi:10.1161/CIRCRESAHA.120.317345.

Machine Learned Cellular Phenotypes Predict Outcome in Ischemic Cardiomyopathy

Albert J. Rogers[1,*], **Anojan Selvalingam**[1,2,*], **Mahmood I. Alhusseini**[1], **David E. Krummen**[3], **Cesare Corrado**[4], **Firas Abuzaid**[5], **Tina Baykaner**[1], **Christian Meyer**[2], **Paul Clopton**[1], **Wayne Giles**[6], **Peter Bailis**[4], **Steven Niederer**[4], **Paul J. Wang**[1], **Wouter-Jan Rappel**[7], **Matei Zaharia**[5], **Sanjiv M. Narayan**[1]

[1]Department of Medicine and Cardiovascular Institute, Stanford University, Stanford, USA

[2]Department of Cardiology, University Medical Center Hamburg-Eppendorf, Germany

[3]Department of Medicine, University of California, San Diego, California, USA

[4]Department of Biomedical Engineering, King's College London, London, U.K.

[5]Department of Computer Sciences, Stanford University, Stanford, USA

[6]Department of Physiology and Pharmacology, University of Calgary, Canada

[7]Department of Physics, University of California, San Diego, California, USA.

Abstract

Rationale: Susceptibility to ventricular arrhythmias (VT/VF) is difficult to predict in patients with ischemic cardiomyopathy either by clinical tools or by attempting to translate cellular mechanisms to the bedside.

Objective: To develop computational phenotypes of patients with ischemic cardiomyopathy, by training then interpreting machine learning (ML) of ventricular monophasic action potentials (MAPs) to reveal phenotypes that predict long-term outcomes.

Methods and Results: We recorded 5706 ventricular MAPs in 42 patients with coronary disease (CAD) and left ventricular ejection fraction (LVEF) ≤40% during steady-state pacing. Patients were randomly allocated to independent training and testing cohorts in a 70:30 ratio, repeated K=10 fold. Support vector machines (SVM) and convolutional neural networks (CNN) were trained to 2 endpoints: (i) sustained VT/VF or (ii) mortality at 3 years. SVM provided superior classification. For patient-level predictions, we computed personalized MAP scores as the proportion of MAP beats predicting each endpoint. Patient-level predictions in independent test cohorts yielded c-statistics of 0.90 for sustained VT/VF (95% CI: 0.76-1.00) and 0.91 for mortality (95% CI: 0.83-1.00) and were the most significant multivariate predictors. Interpreting trained SVM revealed MAP morphologies that, using *in silico* modeling, revealed higher L-type calcium current or sodium calcium exchanger as predominant phenotypes for VT/VF.

Address correspondence to: Sanjiv M. Narayan, 780 Welch Road, MC 5773, Stanford CA 94305, Tel: +1 650-7362563, sanjiv1@stanford.edu.

*These authors served as co-first authors

Conclusion: Machine learning of action potential recordings in patients revealed novel phenotypes for long-term outcomes in ischemic cardiomyopathy. Such computational phenotypes provide an approach which may reveal cellular mechanisms for clinical outcomes and could be applied to other conditions.

Graphical Abstract

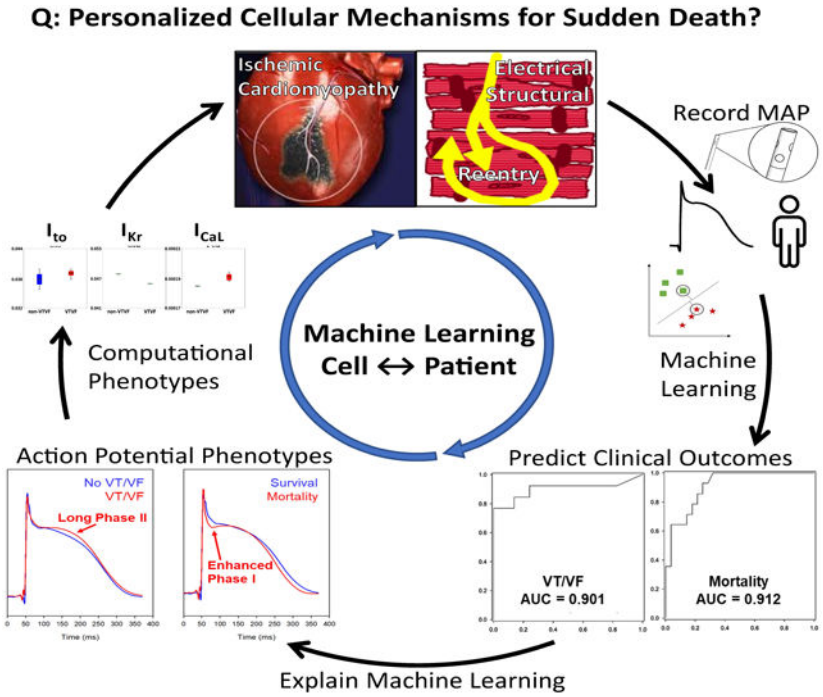

Keywords

Sudden cardiac death; arrhythmia; monophasic action potentials; computational phenotypes; ion channels/membrane transport; artificial intelligence; ischemic cardiomyopathy; systems biology

Subject Terms:

Chronic Ischemic Heart Disease; Computational Biology; Ion Channels/Membrane Transport; Machine learning; Sudden Cardiac Death

INTRODUCTION

Sudden cardiac arrest (SCA) affects over 300,000 individuals per year in the U.S. alone and is a major contributor to healthcare utilization.[1]PP Individuals with reduced left ventricular ejection fraction (LVEF) are at elevated risk for SCA and may qualify for implantable cardiac defibrillators (ICD)s, yet such devices are rarely needed to deliver life-saving therapy in 1 year (< 5-10%)[2] and further risk stratification has proven elusive.[3]

Cellular mechanisms may reveal risk for SCA in inherited conditions, such as specific changes in voltage-gated membrane channels in the long-QT and Brugada syndromes that

correlate with risk for ventricular tachycardia (VT) or fibrillation (VF).[4] However, a cell-to-bedside foundation does not yet exist for broader populations at risk for SCA. In models of heart failure, abnormalities in intracellular calcium homeostasis and in voltage-gated membrane channels[5,6] indicate arrhythmic risk *in vitro*,[7] yet produce complex effects on action potential morphology which have not been translated to clinical care. This may reflect challenges in probing tissue data in patients, or in quantifying those action potential changes that predict specific clinical outcomes.

We hypothesized that the morphology of individual ventricular monophasic action potentials (MAPs) in patients with ischemic cardiomyopathy may identify tissue or cellular electrophysiology phenotypes that can be identified by machine learning and predict long-term outcomes. Franz and colleagues have shown that MAPs accurately reflect transmembrane action potentials in patients.[8] Subsequent studies showed that oscillations in MAPs may increase arrhythmic risk.[9-11] However, it is undefined if the morphology of *in vivo* action potentials, that indicate structural and cellular remodeling including changes in membrane-sensitive ion channels, predict clinical outcome. Machine learning (ML) is a rapidly developing science which has been used to classify data in complex areas including voice recognition, image analysis and game-playing decisions.[12] Clinically, ML can diagnose abnormal heart rhythms from the ECG as well as experts,[13] identify low LVEF from the ECG alone,[14] and uncover immunological phenotypes.[15] ML has been used to predict clinical phenotypes from inputs at the molecular scale.[16] However, ML has yet to be applied to bridge tissue or cellular mechanisms for SCA with clinical outcomes.

We used ML and traditional statistics of MAPs recorded in patients to identify specific ventricular action potential morphologies that predict sustained VT/VF or mortality on long-term follow-up, coupled with biophysical modeling to identify corresponding alterations in cellular electrophysiology, in a well characterized[10,11,17] cohort of individuals with chronic ischemic cardiomyopathy.

METHODS

To enable researchers to verify the results or procedures of the study, non-proprietary software code developed for this project and samples of anonymized data are available at URL: https://github.com/NarayanLab/VT_MAP_Project, as detailed in the Supplemental Materials in sections on Major Resources with Readme documents.

Subject Recruitment.

The study protocol was approved by the Institutional Review Boards of Stanford University and the University of California, San Diego. All subjects provided written informed consent. We recruited 53 patients with LVEF ≤ 40 % and coronary artery disease (CAD) undergoing programmed ventricular stimulation, excluding those with prior sustained ventricular arrhythmias or aborted SCA. All patients were fully revascularized at least three months prior to electrophysiological testing, and antiarrhythmic medications were washed out for > 5 half-lives. We excluded subjects with < 50 high quality MAP tracings due to technical difficulties (N=11). Our resulting population for this study was 42 patients.

Ventricular Pacing at Electrophysiologic Study.

Subjects were studied in the post-absorptive state under conscious sedation with midazolam and fentanyl. In addition to standard catheters, a 7Fr monophasic action potential (MAP) catheter (Boston Scientific, MA) was used to record ventricular action potentials. The MAP catheter measures signals that closely match transmembrane potentials of single cells using a distal exploring hemispherical electrode at its tip and a reference electrode 5mm proximal that removes far-field electrograms.[8] The MAP catheter was advanced transvenously to the apex of the right ventricle (RV, n=37) or, in a minority, via the aorta to the apex of the left ventricle (LV, n=5) with heparin anti-coagulation. Electrophysiological signals were recorded on a physiologic recorder (Bard-Boston Scientific, Marlborough, MA), filtered at 0.05 – 100 Hz (ECG), 0.05-500 Hz (MAPs) and 30-500 Hz (other intracardiac signals) and digitized at 1 kHz.

We performed pacing for 90 seconds at rate of 109 beats/min (cycle length, CL 550ms; IQR: 550-600). Figure 1 illustrates ventricular MAPs, which we recorded at sites of highest regional amplitude to avoid scar and borderzone. Programmed ventricular stimulation was then performed, and considered positive if monomorphic ventricular tachycardia (VT) was induced with 1-3 extrastimuli or polymorphic VT or ventricular fibrillation (VF) were induced with 1-2 extrastimuli. Electrophysiological study was performed under guidelines for ischemic cardiomyopathy with LVEF < 40%, NSVT, and > 90 days from revascularization.[18] Subsequently, ICDs were offered to all patients with LVEF ≤ 35% and were placed in 86% of patients within 2 weeks and 88% of patients overall.

Export of Ventricular Electrogram Data and MAP Preprocessing.

Figure 2 shows data flow in this study. MAP electrograms were exported at 16-bit digital resolution for analysis using custom software (*Python* 3.6). MAP signals were bandpass filtered from 0.5-250 Hz to remove low frequency drift (0.05-0.5 Hz). Analysis focused on each MAP beat as a voltage-time series in a 370 ms window (to encompass the longest MAP[11,17]). MAPs were aligned using the diastolic voltage baseline. Artifactual[8] phase 0 overshoots or undershoots were clipped at 3.0x standard deviation above and below the mean amplitude (Online Figure I).

K-Fold Cross Validation.

Our study design randomly split patients into a 70% cohort for training and an independent 30% cohort for testing. To improve generalizability, we used stratified Monte Carlo cross-validation to evaluate the trained ML classifiers, similar to the approach used by Feeny *et al* for cardiac resynchronization therapy.[19] We performed K-fold cross-validation using K=10, each iteration providing 1 training set and 1 independent test set not used in training. Online Figure II illustrates K splits of data from patients in this project.

Mathematical Features of MAP Morphology.

Individual MAP waveforms were summarized by the tsfresh package (ver. 0.12.0 in *Python* 3.6),[20] which calculates mathematical “features” linked to a defined endpoint (here, VT/VF or mortality in turn). We ranked features by p-values, and removed the least significant using the Benjamini-Yekutieli procedure.[21] Features that correlated highly to one another

(coefficient > 0.9) were represented by the feature with highest p-value to minimize co-linearities. Features were then standardized by the z-score computed using the mean and standard deviation.

To identify the most important features, we implemented logistic regression with L1 regularization on features standardized with z-score transformation, using a regularization factor C = 1 and the 'liblinear' solver in the scikit-learn library (0.21.3). The optimized model was constructed using features with the 40 highest absolute coefficients. The procedure for calculating and filtering features for supervised learning is summarized in Online Figure III and detailed in the Supplemental Methods, which also includes a Glossary of Terms used in this study.

Supervised Machine Learning for Clinical Predictions.

We developed a method to predict patient-level outcomes from raw MAP beats. First, we trained supervised learning models to use a single MAP recording to predict the endpoints of VT/VF or mortality, by training on all beats across patients (beat-level model). Second, because a single MAP may not capture prognostic information in any given patient *in vivo* due to biological or technical variability, we calculated the proportion of each patient's beats classified by the beat-level model to predict the clinical endpoint. The resulting *MAP score* provided a patient-level prediction (Figure 2).

To develop the beat-level model we compared several ML approaches (Supplemental Methods). Support vector machines (SVM) are a data-efficient architecture that can classify complex data from a more limited training dataset than typically required for convolutional neural networks (CNN) or other supervised ML architectures (Online Figure IV, Online Table I).[22] SVM identifies a subset of inputs, termed support vectors, that form a decision boundary that separates output classes (endpoints). Training aims to increase the distance between boundaries and improve generalizability of the model.[22] Extensive testing revealed that SVM provided superior test characteristics to CNN (Online Table II).

Patient-level predictions were made by computing the *MAP score*, that indicates the proportion of test set beats in that patient computed by the beat-level model to predict the endpoint. The MAP score generates a continuous patient-level output as:

$$MAP\ score = \left(\frac{\#\ of\ beats\ predicting\ the\ endpoint}{total\ \#\ of\ beats}\right)$$

for each endpoint in turn.

Prospective Follow-up and Endpoint Labels.

Subjects were followed prospectively for a median of 1290 days (inter-quartile range 920 to 2409) using 4-6 monthly device interrogations, a telephone questionnaire, and reviews of electronic medical records. There was no loss to follow-up. Outcome definitions were (i) VT/VF detected by ICDs programmed uniformly for VT > 170-210 beats/min and VF > 210 beats/min, by analyzing 16/24 intervals on first and 8/12 intervals on subsequent detections. The small number of patients without ICDs had evaluation of VT/VF > 30 s by clinical care

assessments. (ii) All-cause mortality was defined by the death registry. All data were consolidated via a comprehensive electronic medical records system. Endpoints were assigned by 3 senior clinical authors blinded to electrophysiological analyses at the 3-year follow-up in all patients (no censoring).

Physiological Interpretation of Machine Learning.

We analyzed trained SVM models to reveal the electrophysiological properties of beats predicting each endpoint. We computed: (i) the arithmetic mean of all MAP beats (in a 370 ms window) that predicted VT/VF versus those predicting no VT/VF, and (ii) the arithmetic mean of MAP beats that predicted mortality versus those that predicted survival. MAPs were aligned by phase 0 upstrokes.

Biophysical cardiac cell modeling provides a framework to quantitatively link ionic pathways (channels, exchangers and pumps) through to action potential morphology. We used the O'Hara myocyte model, validated in human ventricles and recommended by the Food and Drug Administration for drug testing for SCA,[23] to investigate changes in ionic pathway density for MAPs measured to predict VT/VF or mortality. A 2-stage process was applied. First, we studied the 5 ionic pathway alterations reported to be most important in heart failure.[24] This includes the hERG channel (I_{Kr}), L-Type Ca^{2+} Channel (I_{CaL}), Na^{+}-Ca^{2+} exchanger (NCX), Transient Outward current (I_{to}) and sarcoplasmic reticulum ATPase (SERCA). We discretized these pathways over 21 increments in a range of −80% to +100% of default values, providing 21^5 = 4,084,101 parameter sets. This generated a complete data set for all possible action potentials over this range of conductances for these 5 ionic pathways. Second, we performed a global sensitivity analysis to identify the pathways that produced action potentials that best matched mean recorded MAP durations at 30, 60, and 90% repolarization for each endpoint.[25-27]

Detailed modeling methods are provided in Supplemental Methods.

Statistical Analysis.

Normality was evaluated using the Kolmogorov-Smirnov test. Continuous clinical data, respiratory rates, and autocorrelation quality indices are represented as mean ± standard deviation or as median (quartiles) and compared with t-tests or Mann-Whitney U tests as appropriate. Nominal variables are compared with Fisher exact tests. Predictions from SVM model test sets are reported as overall accuracy and confusion matrices. We performed receiver operating characteristic (ROC) analysis of MAP scores and defined the optimal cut-point as the point closest to the upper-left corner and calculated the area under the curve (AUC). Applying the optimum cut-point to MAP scores allowed us to identify patients at low and high risk for each endpoint, and calculate decision statistics (sensitivity, specificity, positive and negative predictive values, and accuracy). The binary MAP score groups were included in univariate and multivariate logistic regression analyses. Multivariate tests were conducted using stepwise selection, setting p-values of 0.05 to enter and 0.10 to remove variables. For supplemental confirmation, we performed multivariate testing that included covariates with $p < 0.10$ in univariate testing. Spearman's correlation was used to evaluate the association between VT/VF and mortality MAP scores. A probability of < 0.05 was

considered statistically significant. All tests are 2-sided and no adjustments for multiple comparisons were employed.

RESULTS

The baseline characteristics of subjects are shown, separated by the primary endpoint of VT/VF (Table 1) or mortality (Online Table III) on 3-year follow-up. A total of 5706 MAPs were available in this study, and each patient provided 136 ± 92 MAP signals for analysis.

On follow-up of > 3 years, 13 patients had sustained ventricular arrhythmias and 14 patients died. Patients with and without events had similar LVEF, age and other demographics for the endpoints of VT/VF (Table 1) or mortality (Online Table III). Prevalence of devices in follow up (88% overall) did not differ between patients with and without VT/VF ($p = 0.30$), or those who died versus those who survived ($p = 1.0$). On electrophysiological testing, ventricular arrhythmias were inducible in N=14 patients while N=28 patients were non-inducible. There were no differences in patient demographics separated according to inducibility (Online Table IV). There were no differences in time from revascularization in patients with/without events for each endpoint.

Mathematical Features of MAPs.

The top 40 features extracted by *tsfresh* from the entire dataset are shown grouped for the endpoints of VT/VF (Online Table V) and mortality (Online Table VI). Features were found to represent frequency domain and mathematical indices of action potential shape.

Analysis of Single Beats and Creation of MAP scores.

Predictive accuracy of the SVM for single beats (beat-level analysis) was 83.2% (CI: 82.6 - 83.8%) for VT/VF and 75.4% (CI: 74.7-76.0%) for mortality. Online Table VII presents full test characteristics. Extensive testing showed that the SVM model outperformed CNN models for both endpoints (Online Table I).

MAP scores provide a continuous output for each patient less affected by variability in a single MAP waveform (patient-level analysis). The mean VT/VF MAP score was 0.31 ± 0.33 and the mean mortality MAP score was 0.34 ± 0.31. Across patients, MAP scores for both endpoints were uncorrelated ($r=0.05$, $p=0.78$), suggesting that separate characteristics of MAP shape predicted each endpoint.

MAPs did not differ between patients who did or did not experience events based on artifact from respiratory rate (Online Table VIII) or estimates of overall MAP signal quality (Online Table IX) for either endpoint.

Patient-Level Prediction of Sustained VT/VF and Mortality.

Of the 42 patients, 13 experienced sustained VT/VF. Figure 3A shows the ROC curve generated by varying the cut point for the MAP score for the VT/VF endpoint. The area under the curve (AUC) for this metric was 0.90 (95% CI = 0.76-1.00). The optimal cut-point yielded an accuracy of 85.7%.

The causes of mortality in our population were cardiac or unexplained (n=11), renal failure (n=1), malignancy (n=1) or sepsis (n=1). Figure 3B shows the ROC curve for the MAP score related to the mortality endpoint, for which the AUC was 0.91 (95% CI: 0.83-1.00). The optimal cut point yielded an accuracy of 81.0%. Decision statistics (clinical predictive indices) for both VT/VF and mortality are summarized in Table 2.

Deriving Pathophysiological Phenotypes from Machine Learning.

Machine learning is often considered to be a 'black box'. To address this, we set out to identify MAP shapes predicting each endpoint. Figure 4A shows average MAP shapes that predicted sustained VT/VF versus those that predicted no VT/VF by the trained SVM. MAP waveforms that predicted VT/VF had higher plateau height (0.969 ± 1.34 vs. 0.839 ± 1.74 standardized mV, $p < 0.001$) and longer phase II duration (176 ± 35 ms vs 163 ± 40 ms, $p < 0.001$) compared to MAPs that did not.

Figure 4B shows average MAP shapes that predicted mortality versus those that predicted survival by the trained SVM. We quantified phase I as the mean voltage of each MAP from the upstroke to phase II, between 10ms to 40ms after phase 0. For MAP beats that predicted mortality, the mean Phase I standardized voltage was lower than in those predicting survival (2.44 ± 1.31 vs. 3.32 ± 2.47, $p < 0.001$). This phase I metric predicted mortality with a c-statistic of 0.816 (CI: 0.676 to 0.957).

Conversely, examining phase 0 upstroke velocity, the maximum dV/dt for MAP recordings poorly separated patients with and without endpoints (c-statistic 0.605 for VT/VF, 0.625 for mortality). Action potential durations at 90% repolarization (APD90) did not separate patients with and without VT/VF (262 ± 31 vs 249 ± 39 ms; $p = 0.30$) nor mortality (250 ± 42 vs. 259 ± 24 ms, respectively; $p = 0.34$).

We next studied potential ionic pathways explaining each MAP phenotype. *Biophysical cell models* showed that all 5 ionic pathways contributed to APD in the FDA-approved O'Hara model (Figure 5). Global sensitivity analysis revealed that SERCA had the smallest contribution (Figure 5A). We thus considered 2 datasets of ionic pathways made up of $I_{Kr,}$ I_{to} and either (a) I_{CaL} or (b) NCX, which both cause a depolarizing current and have similar importance to APD (Figure 5A).

We found that higher I_{CaL} (Figure 5B) or enhanced NCX (Figure 5C) resulted in increased action potential plateau height and duration in MAPs that predicted VT/VF compared with those that did not. To study pro-arrhythmia, we found that APD alternans arose more often in models with higher I_{CaL} than those with lower I_{CaL} at slow pacing rates (36.25% vs. 2.5% of simulations at cycle lengths ≥ 220 ms), but similar prevalence at faster rates (23.75% vs. 30.25% at cycle lengths < 220 ms). APD alternans had similar prevalence in cell models with enhanced or non-enhanced NCX at both rates (50.0% vs 52.5%, and 25% vs 32.0%, respectively). Differences in I_{Kr} were also found, consistent with the small non-significant differences in measured APD.

Patients who died, compared to those who survived, showed action potentials with increased I_{Kr} conductance or minor reduction in NCX that fit to measured differences in APD90 (Figure 5B and 5C). These cellular investigations are detailed in Supplementary results.

Prediction of Endpoints by Logistic Regression Analyses.

Table 3 shows the results of univariate and multivariate logistic regression analyses. For the VT/VF endpoint, the MAP score yielded a univariate odds ratio of 26.4 (CI: 4.4-157.9, $p < 0.001$) and was the predominant predictor in the multivariate model. No potential covariate met the criterion of $p < 0.10$ for inclusion in the multivariate model. Neither testing for induction of VT/VF, nor the presence of ICD within 14 days of testing, nor coronary artery disease distributions from angiography predicted VT/VF. For the mortality endpoint, the MAP score yielded a univariate odds ratio of 22.0 (CI: 3.8-126.4, $p = 0.001$). This result remained significant in the stepwise test where the odds ratio was 31.0 (CI: 3.2-299.0, $p=0.003$) and when age, pre-procedural beta blocker use, and log BNP were forced into the model the odds ratio was 30.8 (CI: 2.6-361.5, $p=0.006$).

DISCUSSION

Our study supports the hypothesis that patients with ischemic cardiomyopathy exhibit tissue and cellular phenotypes that predict outcome. Machine learning of ventricular action potentials recorded in patients with ischemic cardiomyopathy, combined with extensive *in silico* analysis of ionic pathways, revealed electrophysiological phenotypes that predicted long-term vulnerability to VT/VF or mortality. These computational phenotypes improved upon the predictive value of traditional clinical risk markers in independent test cohorts. Future studies could extend our results to body surface ECGs or device-acquired signals for wider screening. By linking cellular physiology with clinical outcomes, this computational phenotyping approach may have promise for mechanism-guided management of other conditions.

Using Electrophysiologic Remodeling to Predict SCA.

Although LVEF < 35% is a guideline for ICD implantation, this index of mechanical remodeling has suboptimal sensitivity and specificity for SCA.[3] This is particularly true for patients with LVEF 35-40%, who we included in our study and in whom risk stratification is difficult even including electrophysiologic testing.

Our study reveals that MAPs with a more depolarized and prolonged phase II predicted risk for sustained VT/VF, and outperformed LVEF and other clinical predictors. Although the magnitude of MAP changes were small, relatively small changes in action potential plateau have been shown to produce large changes in I_{CaL} and large increases in contractility.[28]

Our action potential simulations revealed that increased I_{CaL} or enhanced NCX can explain this augmented height and prolonged Phase II plateau, with APD alternans in I_{CaL} models supporting a pro-arrhythmic role. Modulation of the L-type Ca^{2+} current has not previously been reported to convey risk for VT/VF in patients with ischemic cardiomyopathy. However, increased I_{CaL} is an established mechanism for ventricular arrhythmias in heart failure related to increased beta-adrenergic tone,[29] and in patients with LQTS,[6] BrS,[30] and early

repolarization syndromes.[31] The effect of enhanced NCX is consistent with increased intracellular calcium from elevated I_{CaL}. Direct tissue biopsy could further dissect these mechanisms for VT/VF, as well as potential contributions of fibrosis or ultrastructural connexin abnormalities.[32]

Clinical recordings showed that MAPs from patients who died showed enhanced early repolarization (phase I) compared to those who survived, and no significant differences in APD. Whether our observed changes in phase I reflect altered I_{to} requires further study. Our computational models, while used by the FDA to screen risk for sudden death[23], emphasize APD and mechanisms of repolarization reserve and under-emphasize phase I repolarization which is of short duration.[33] Increased I_{to} has a plausible mechanistic role in patients with ischemic cardiomyopathy, and is linked with adverse outcomes in patients with Brugada syndrome,[30] J wave syndromes,[31] and as a cause of early afterdepolarizations in animal models.[34] I_{to} current is higher in right than left ventricle, at the apex versus the base,[35] and interacts with I_{CaL} to cause a repolarization notch in MAP tracings.[36]

Potentially differing mechanisms for VT/VF and mortality are consistent with the opposite APD effects observed, albeit small in magnitude, for patients with or without VT/VF compared to patients with or without mortality. Hypothetically, APD lengthening could explain VT/VF by reentry, particularly if spatially heterogeneous. APD shortening could explain mortality by factors such as inflammation or frailty, and patients who died were indeed older at recruitment, with higher BNP and a trend for lower potassium (Online Table III). Changes in APD must be considered in the context of the other observed waveform alterations.

Whether our tissue recording patterns in individual patients reflect changes in net repolarizing current at the myocyte level requires confirmation in biopsy specimens; or perhaps through the use of induced pluripotential stem cells,[37] or gene therapy,[32] guided by established principles of all-or-none repolarization.[5]

Using Machine Learning to Predict SCA.

ML has not previously been applied to identify cellular phenotypes for arrhythmias. Ramirez et al. applied SVM to the rate response of repolarization on the ECG 0T0Tto identify patients who may suffer SCA versus death from heart failure.[38] Lee et al. trained neural networks using heart rate variability from 52 0T0TECG tracings prior to arrhythmia and 52 control tracings. Their approach 0T0Tpredicted imminent sustained VT (within 1 hour)0T0T[39]0T0T but did not predict long-term outcomes0T0T. Aro *et al.* used ML to identify 14 ECG parameters that predicted SCA in large cohorts[40] and Lyon *et al.*[41] identified novel ECG and structural clusters which may predict SCA in patients with hypertrophic cardiomyopathy.

In developing ML to partition action potential shapes to predict SCA, we compared several model architectures and found that SVM performed better than CNN-based models. CNNs perform optimally by linking features in time-series data, which are high dimensional, and may be considered data hungry. Conversely, SVM can operate on features of lower dimensionality,[22] which may explain their performance here. Studies to define optimal ML

and statistical approaches to classify tissue-level and whole heart electrophysiologic data are ongoing in our laboratory.

Comparison with Traditional Predictors of Long-term Outcomes.

Our predictive model outperformed traditional clinical predictors. Prior studies confirm that inducible arrhythmias at programmed stimulation modestly predict long-term outcomes in patients with ischemic cardiomyopathy.[42] LVEF alone is a poor predictor of sudden cardiac death with a c-statistic of 0.57 that may improve little (to 0.64) by adding other clinical data.[43] Comorbidities such as worse NYHA class, atrial fibrillation, and non-sustained VT confer higher risk,[42] yet also increase the proportion of non-arrhythmic deaths. Oscillations of intracardiac electrograms or the ECG T-wave[9-11,44] prolonged ECG QRS duration or clinical comorbidities are insufficiently predictive to guide therapy.[2] As with all predictive models, the use of our MAP-based model requires consideration of other clinical indicators.

Clinical Implications.

Computational phenotyping which links cellular and tissue-level data with clinical outcomes could provide a basis for mechanism-based personalized management. This multidisciplinary approach could be broadened using non-invasive ECG imaging of epicardial unipolar electrograms[45] or device-acquired unipolar ventricular electrograms, which show similarities in shape and rate response to MAPs.[46] Cellular phenotypes could be refined using tissue biopsy samples, or potentially induced pluripotential stem cells, from patients in low and high-risk groups. The utility and reliability of machine learning could be enhanced by incorporating well-labeled biomarker, genomic and clinical data to the models. With further development, cellular phenotypes may form the basis to identify high- and low-risk clinical groups, to guide patient-level therapy, for drug discovery, or to repurpose existing medications.

Limitations.

Our patient cohort was relatively small. On the other hand, this dataset of 5706 MAPs in 42 patients (with long term follow-up) is also among the largest that has been reported. Ideally, we would have confirmed cellular phenotypes by tissue biopsy, but there was no clinical indication for cardiac biopsy in these patients.

MAPs were not sampled spatially within the ventricles, although our study design ensures that recordings were standardized in anatomical location to increase reproducibility. The relationship of MAP recordings to ventricular scar was not defined, although relatively large and stable MAP amplitudes ruled out substantial scar or border zone effect.[47] While successive MAPs within a patient may vary, we quantified this using our MAP score approach. Future work should address regional MAP variation across each ventricle, compared between right and left ventricles, and studied in relation to MRI-determined scar. This could also be attempted using MAP surrogates from body surface ECG imaging, or ultimately by *in vivo* optical imaging.[48]

Patients in this study were predominantly male, and future work should address gender-specific effects and differences. Patients underwent electrophysiologic study, but there was

no detected statistical bias introduced by the presence of implanted devices, since 88% received ICDs in follow-up (most within 2 weeks of EPS).

Conclusions.

Machine learning of ventricular monophasic action potential recordings combined with cellular biophysical analyses revealed electrophysiologic phenotypes that predicted long-term outcomes in patients with ischemic cardiomyopathy. This computational phenotyping approach outperformed established clinical predictors and, with further development, could facilitate mechanism-guided management of other diseases.

Supplementary Material

Refer to Web version on PubMed Central for supplementary material.

Acknowledgments

SOURCES OF FUNDING

Dr. Rogers acknowledges research funding from NIH (F32 HL144101). The doctoral research fellowship of Anojan Selvalingam is funded by the Hans-Boeckler-Foundation, sponsored by the German Federal Ministry of Education and Research. Dr. Baykaner acknowledges funding from NIH (K23 HL145017). Dr. Rappel reports research grants from the NIH (R21 HL145500, R01 HL122384). Dr Niederer and Dr Corrado are funded by UK Engineering and Physical Sciences Research Council (EP/P01268X/1). Dr. Narayan reports research grants from NIH (R01 HL83359, R01 HL149134).

DISCLOSURES

Mr. Alhusseini reports intellectual property rights from Stanford University. Dr. Niederer reports intellectual property rights from King's College London and support from Siemens, Pfizer, EBR systems, Boston Scientific, and Abbott (all modest). Dr. Wang reports fellowship support from Biosense-Webster, Boston Scientific, Medtronic, and Abbott (all modest). Dr. Rappel reports intellectual property rights from the University of California Regents. Dr. Matei Zaharia and Dr. Peter Bailis acknowledge affiliate members and other supporters of the Stanford DAWN project---Ant Financial, Cisco, Facebook, Google, Infosys, Intel, Microsoft, NEC, SAP, Teradata, and VMware---as well as Toyota Research Institute, Keysight Technologies, Amazon Web Services, and the NSF under CAREER grant CNS-1651570. Dr. Narayan reports consulting from Beyond.ai Inc, TDK Inc., Up to Date, Abbott Laboratories, and American College of Cardiology Foundation (all modest); Intellectual Property Rights from University of California Regents and Stanford University.

Nonstandard Abbreviations and Acronyms:

MAP	Monophasic action potential
ML	Machine learning
ICD	Implantable cardioverter defibrillator
SVM	Support vector machines
CNN	Convolutional neural network
I_{Kr}	hERG channel current
I_{CaL}	L-Type Ca^{2+} Channel current
I_{to}	Transient outward potassium current

NCX	Na^+-Ca^{2+} exchanger
SERCA	Sarcoplasmic reticulum ATPase
APD[XX]	Action potential duration at (XX%) repolarization

REFERENCES

1. Benjamin EJ, Virani SS, Callaway CW, et al. Heart Disease and Stroke Statistics—2018 Update: A Report From the American Heart Association. Circulation. 2018;137:E67–E492. [PubMed: 29386200]
2. Goldberger JJ, Basu A, Boineau R, et al. Risk Stratification for Sudden Cardiac Death: A Plan for the Future. Circulation. 2014;129:516–526. [PubMed: 24470473]
3. Waks JW, Buxton AE. Risk Stratification for Sudden Cardiac Death After Myocardial Infarction. Annu Rev Med. 2018;69:147–164. [PubMed: 29414264]
4. Zhang Y, Guallar E, Blasco-Colmenares E, et al. Clinical and Serum-Based Markers Are Associated with Death within 1 Year of de Novo Implant in Primary Prevention ICD Recipients. Heart Rhythm. 2015;12:360–366. [PubMed: 25446153]
5. Trenor B, Cardona K, Saiz J, Noble D, Giles W. Cardiac Action Potential Repolarization Revisited: Early Repolarization Shows All-or-None Behaviour. J Physiol. 2017;595:6599–6612. [PubMed: 28815597]
6. Skinner JR, Winbo A, Abrams D, Vohra J, Wilde AA. Channelopathies That Lead to Sudden Cardiac Death: Clinical and Genetic Aspects. Hear Lung Circ. 2019;28:22–30.
7. Narayan SM, Wang PJ, Daubert JP. New Concepts in Sudden Cardiac Arrest to Address an Intractable Epidemic: JACC State-of-the-Art Review. J Am Coll Cardiol. 2019;73:70–88. [PubMed: 30621954]
8. Franz MR, Burkhoff D, Spurgeon H, Weisfeldt ML, Lakatta EG. In Vitro Validation of a New Cardiac Catheter Technique for Recording Monophasic Action Potentials. Eur Heart J. 1986;7:34–41. [PubMed: 2420597]
9. Narayan SM, Kim J, Tate C, Berman BJ. Steep Restitution of Ventricular Action Potential Duration and Conduction Slowing in Human Brugada Syndrome. Heart Rhythm. 2007;4:1087–1089. [PubMed: 17675086]
10. Narayan SM, Bayer JD, Lalani G, Trayanova NA. Action Potential Dynamics Explain Arrhythmic Vulnerability in Human Heart Failure. J Am Coll Cardiol. 2008;52:1782–1792. [PubMed: 19022157]
11. Bayer JD, Lalani GG, Vigmond EJ, Narayan SM, Trayanova NA. Mechanisms Linking Electrical Alternans and Clinical Ventricular Arrhythmia in Human Heart Failure. Heart Rhythm. 2016;13:1922–1931. [PubMed: 27215536]
12. Jaderberg M, Czarnecki WM, Dunning I, et al. Human-Level Performance in 3D Multiplayer Games with Population-Based Reinforcement Learning. Science. 2019;364:859–865. [PubMed: 31147514]
13. Hannun AY, Rajpurkar P, Haghpanahi M, Tison GH, Bourn C, Turakhia MP, Ng AY. Cardiologist-Level Arrhythmia Detection and Classification in Ambulatory Electrocardiograms Using a Deep Neural Network. Nat Med. 2019;25:65–69. [PubMed: 30617320]
14. Attia ZI, Kapa S, Lopez-Jimenez F, et al. Screening for Cardiac Contractile Dysfunction Using an Artificial Intelligence–Enabled Electrocardiogram. Nat Med. 2019;25:70–74. [PubMed: 30617318]
15. Sweatt AJ, Hedlin HK, Balasubramanian V, et al. Discovery of Distinct Immune Phenotypes Using Machine Learning in Pulmonary Arterial Hypertension. Circ Res. 2019;124:904–919. [PubMed: 30661465]
16. Yang P-C, DeMarco KR, Aghasafari P, et al. A Computational Pipeline to Predict Cardiotoxicity. Circ Res. 2020;126:947–964. [PubMed: 32091972]

17. Narayan SM, Franz MR, Lalani G, Kim J, Sastry A. T-Wave Alternans, Restitution of Human Action Potential Duration, and Outcome. J Am Coll Cardiol. 2007;50:2385–2392. [PubMed: 18154963]
18. Al-Khatib SM, Stevenson WG, Ackerman MJ, et al. 2017 AHA/ACC/HRS Guideline for Management of Patients With Ventricular Arrhythmias and the Prevention of Sudden Cardiac Death. vol. 138 2018.
19. Feeny AK, Rickard J, Patel D, et al. Machine Learning Prediction of Response to Cardiac Resynchronization Therapy. Circ Arrhythm Electrophysiol. 2019;12:e007316. [PubMed: 31216884]
20. Christ M, Braun N, Neuffer J, Kempa-Liehr AW. Time Series Feature Extraction on Basis of Scalable Hypothesis Tests (Tsfresh – A Python Package). Neurocomputing. 2018;307:72–77.
21. Yekutieli D, Benjamini Y. The Control Of The False Discovery Rate In Multiple Testing Under Dependency. Ann Stat. 2001;29:1165–1188.
22. Nalepa J, Kawulok M. Selecting Training Sets for Support Vector Machines: A Review. Artif Intell Rev. 2019;52:857–900.
23. O'Hara T, Virág L, Varró A, Rudy Y. Simulation of the Undiseased Human Cardiac Ventricular Action Potential: Model Formulation and Experimental Validation. PLoS Comput Biol. 2011;7:e1002061. [PubMed: 21637795]
24. Walmsley J, Rodriguez JF, Mirams GR, Burrage K, Efimov IR, Rodriguez B. MRNA Expression Levels in Failing Human Hearts Predict Cellular Electrophysiological Remodeling: A Population-Based Simulation Study. PLoS One. 2013;8:e56359. [PubMed: 23437117]
25. Laleg-Kirati TM, Crépeau E, Sorine M. Semi-Classical Signal Analysis. Math Control Signals, Syst. 2013;25:37–61.
26. Saltelli A, Annoni P, Azzini I, Campolongo F, Ratto M, Tarantola S. Variance Based Sensitivity Analysis of Model Output. Design and Estimator for the Total Sensitivity Index. Comput Phys Commun. 2010;181:259–270.
27. Ishigami T, Homma T. An Importance Quantification Technique in Uncertainty Analysis for Computer Models. [1990] Proceedings. First Int. Symp. Uncertain. Model. Anal., IEEE Comput. Soc. Press; 1990, p. 398–403.
28. Nathan D, Beeler GW. Electrophysiologic Correlates of the Inotropic Effects of Isoproterenol in Canine Myocardium. J Mol Cell Cardiol. 1975;7:1–15. [PubMed: 1121029]
29. Johnson DM, Antoons G. Arrhythmogenic Mechanisms in Heart Failure: Linking β-Adrenergic Stimulation, Stretch, and Calcium. Front Physiol. 2018;9:1–23. [PubMed: 29377031]
30. Zhang J, Sacher F, Hoffmayer K, et al. Cardiac Electrophysiological Substrate Underlying the ECG Phenotype and Electrogram Abnormalities in Brugada Syndrome Patients. Circulation. 2015;131:1950–1959. [PubMed: 25810336]
31. Antzelevitch C, Yan GX. J Wave Syndromes. Heart Rhythm. 2010;7:549–558. [PubMed: 20153265]
32. Greener ID, Sasano T, Wan X, Igarashi T, Strom M, Rosenbaum DS, Donahue JK. Connexin43 Gene Transfer Reduces Ventricular Tachycardia Susceptibility after Myocardial Infarction. J Am Coll Cardiol. 2012;60:1103–1110. [PubMed: 22883636]
33. Mirams GR, Davies MR, Brough SJ, Bridgland-Taylor MH, Cui Y, Gavaghan DJ, Abi-Gerges N. Prediction of Thorough QT Study Results Using Action Potential Simulations Based on Ion Channel Screens. J Pharmacol Toxicol Methods. 2014;70:246–254. [PubMed: 25087753]
34. Zhao Z, Xie Y, Wen H, et al. Role of the Transient Outward Potassium Current in the Genesis of Early Afterdepolarizations in Cardiac Cells. Cardiovasc Res. 2012;95:308–316. [PubMed: 22660482]
35. Boukens BJD, Christoffels VM, Coronel R, Moorman AFM. Developmental Basis for Electrophysiological Heterogeneity in the Ventricular and Outflow Tract Myocardium as a Substrate for Life-Threatening Ventricular Arrhythmias. Circ Res. 2009;104:19–31. [PubMed: 19118284]
36. Viitasalo M, Paavonen KJ, Swan H, Kontula K, Toivonen L. Effects of Epinephrine on Right Ventricular Monophasic Action Potentials in the LQT1 Versus LQT2 Form of Long QT

Syndrome: Preferential Enhancement of “Triangulation” in LQT1. PACE. 2005;28:219–227. [PubMed: 15733182]

37. Wu JC, Garg P, Yoshida Y, Yamanaka S, Gepstein L, Hulot JS, Knollmann BC, Schwartz PJ. Towards Precision Medicine With Human IPSCs for Cardiac Channelopathies. Circ Res. 2019;125:653–658. [PubMed: 31465267]
38. Ramírez J, Monasterio V, Mincholé A, et al. Automatic SVM Classification of Sudden Cardiac Death and Pump Failure Death from Autonomic and Repolarization ECG Markers. J Electrocardiol. 2015;48:551–557. [PubMed: 25912974]
39. Lee H, Shin SY, Seo M, Nam GB, Joo S. Prediction of Ventricular Tachycardia One Hour before Occurrence Using Artificial Neural Networks. Sci Rep. 2016;6:1–7. [PubMed: 28442746]
40. Aro AL, Reinier K, Rusinaru C, et al. Electrical Risk Score beyond the Left Ventricular Ejection Fraction: Prediction of Sudden Cardiac Death in the Oregon Sudden Unexpected Death Study and the Atherosclerosis Risk in Communities Study. Eur Heart J. 2017;38:3017–3025. [PubMed: 28662567]
41. Lyon A, Ariga R, Mincholé A, et al. Distinct ECG Phenotypes Identified in Hypertrophic Cardiomyopathy Using Machine Learning Associate With Arrhythmic Risk Markers. Front Physiol. 2018;9:1–13. [PubMed: 29377031]
42. Zeitler EP, Al-Khatib SM, Friedman DJ, et al. Predicting Appropriate Shocks in Patients with Heart Failure: Patient Level Meta-Analysis from SCD-HeFT and MADIT II. J Cardiovasc Electrophysiol. 2017;28:1345–1351. [PubMed: 28744959]
43. Reinier K, Narayanan K, Uy-Evanado A, Teodorescu C, Chugh H, Mack WJ, Gunson K, Jui J, Chugh SS. Electrocardiographic Markers and Left Ventricular Ejection Fraction Have Cumulative Effects on Risk of Sudden Cardiac Death. JACC Clin Electrophysiol. 2015;1:542–550. [PubMed: 26949741]
44. Verrier RL, Klingenheben T, Malik M, et al. Microvolt T-Wave Alternans: Physiological Basis, Methods of Measurement, and Clinical Utilityconsensus Guideline by International Society for Holter and Noninvasive Electrocardiology. J Am Coll Cardiol. 2011;58:1309–1324. [PubMed: 21920259]
45. Cuculich PS, Schill MR, Kashani R, et al. Noninvasive Cardiac Radiation for Ablation of Ventricular Tachycardia. NEJM. 2017;377:2325–2336. [PubMed: 29236642]
46. Yue AM, Paisey JR, Robinson S, Betts TR, Roberts PR, Morgan JM. Determination of Human Ventricular Repolarization by Noncontact Mapping: Validation with Monophasic Action Potential Recordings. Circulation. 2004;110:1343–1350. [PubMed: 15353505]
47. Chinyere IR, Hutchinson M, Moukabary T, Lancaster J, Goldman S, Juneman E. Monophasic Action Potential Amplitude for Substrate Mapping. Am J Physiol - Hear Circ Physiol. 2019;317:H667–H673.
48. Lee P, Quintanilla JG, Alfonso-Almazán JM, et al. In Vivo Ratiometric Optical Mapping Enables High-Resolution Cardiac Electrophysiology in Pig Models. Cardiovasc Res. 2019;115:1659–1671. [PubMed: 30753358]

NOVELTY AND SIGNIFICANCE

What Is Known?

- Patients with ischemic cardiomyopathy are at increased risk for sudden cardiac arrest
- Structural and electrophysiological remodeling occur at the cellular level in these patients, but it is unclear which aspects of cellular electrophysiology contribute to clinical events.

What New Information Does This Article Contribute?

- Machine learning of ventricular action potential shape in patients with ischemic cardiomyopathy revealed cellular electrophysiologic phenotypes which predicted future sudden death.
- Long term arrhythmic risk was predicted by prolonged phase II repolarization, reflecting abnormal calcium handling in computational models, while long term mortality was predicted by enhanced early repolarization in ventricular myocardium.
- Machine learning to classify complex physiological data, then probing machines to reveal novel disease phenotypes, represents a novel pipeline that bridges cellular mechanisms to clinical outcomes

Patients with ischemic cardiomyopathy are at elevated risk for sudden cardiac arrest, but further risk stratification has remained challenging. A link from basic electrophysiology phenotypes to clinical outcomes exists for certain inherited cardiomyopathies, but not yet for more general populations with heart disease. Using physiologic recordings from patient's hearts, we trained a machine learning model to predict clinical outcomes in patients with ischemic cardiomyopathy. By careful interrogation of the trained machines, we found cellular phenotypes linked with elevated risk of ventricular arrhythmias and death. Abnormal calcium handling and a prolonged phase II repolarization lead to increased ventricular arrhythmias. Enhanced early repolarization pattern portended risk for mortality. This pipeline of machine learning, interrogation of trained machines, and discovery of new physiology with clinical impact may bridge basic scientific understanding to other important clinical entities.

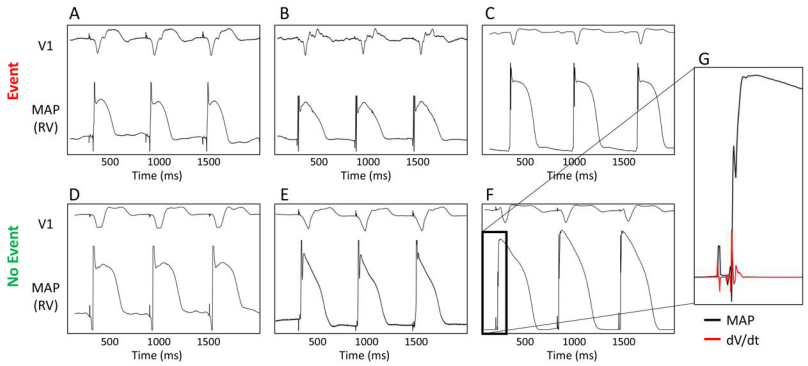

Figure 1.

Ventricular monophasic action potentials (MAPs) in patients with ischemic LV dysfunction with (top row) or without (bottom row) events on long-term follow-up. Panels show (A) 79-year-old male, LVEF 29% with appropriate ICD therapy at 400 days; (B) 55-year-old male, LVEF 35% with ICD therapy at 598 days; (C) 70-year-old male, LVEF 25% who died from congestive heart failure at 95 days. Bottom panels show (D) 45-year-old female, LVEF 26%, (E) 63-year-old male, LVEF 40%, (F) 59-year-old male, LVEF 21%, each of whom had no event at > 3 years of follow-up. (G) Expanded MAP upstroke from patient in (F) (black) with dV/dt (red) illustrating signal fidelity.

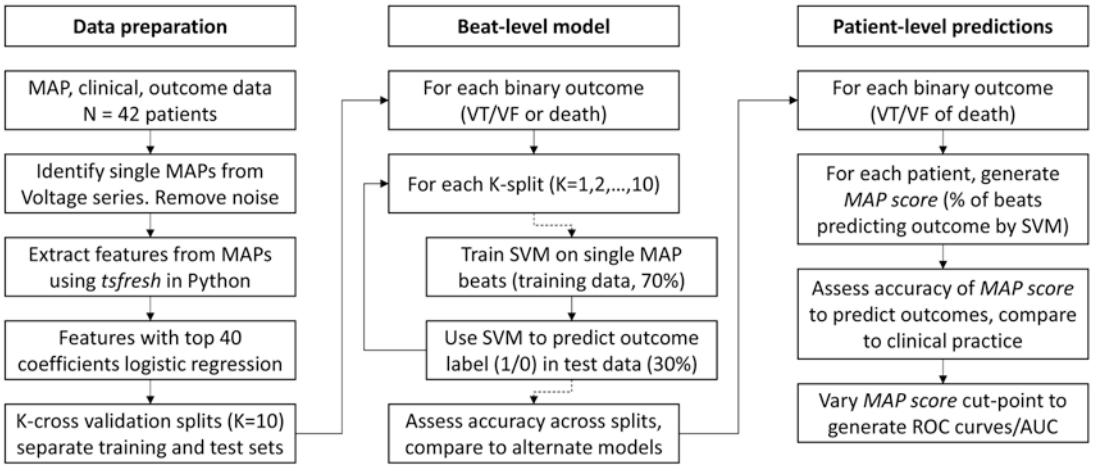

Figure 2.
Data flow in study.

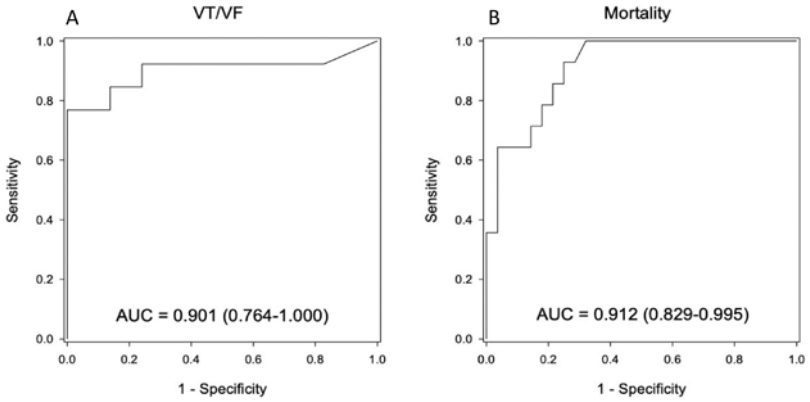

Figure 3.

Receiver operating characteristics of patient-level MAP scores for (A) sustained VT/VF and (B) all-cause mortality on 3-year follow-up.

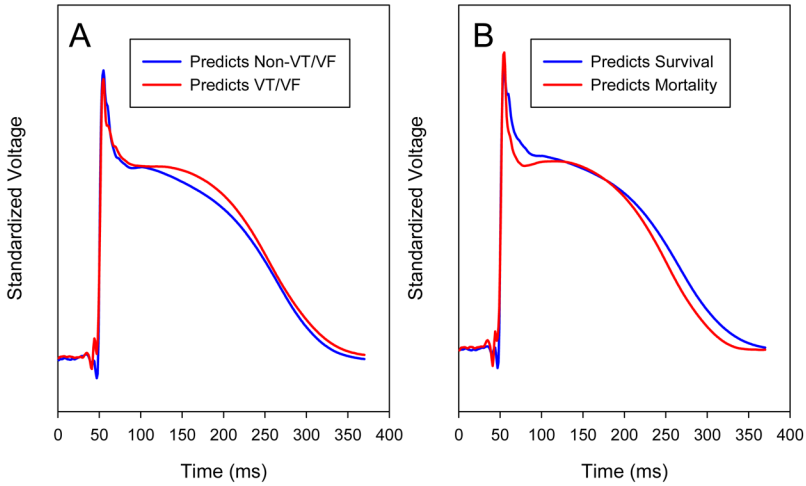

Figure 4. MAP Morphologies identified by Machine Learning to predict endpoints of (a) VT/VF and (b) overall mortality.

a. Average computed from all single beats that predicted VT/VF (red) or no VT/VF (blue).

b. Average computed from all single beats that predicted mortality (red) or survival (blue).

Means were computed from SVM results for all 10 folds in learn and test sets combined.

Voltages are standardized within each curve and adjusted for small offsets at time zero.

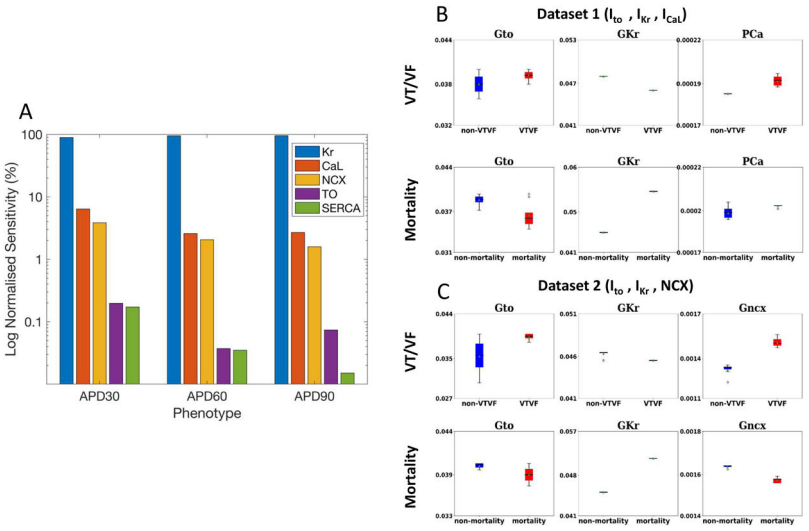

Figure 5. Cellular Biophysical Simulations Probe How Machine Learning of MAPs Predicted Clinical Outcomes.

A) Global sensitivity analysis of the contribution of I_{kr} (Kr), I_{CaL} (CaL), NCX, I_{to} (TO) and SERCA, which are altered in heart failure[24]. The vertical scale is the normalized sensitivity (%) of action potential durations at 30% (APD30), 60% (APD60) and 90% (APD90) repolarization to each pathway (log scale). B) Ionic pathway densities for dataset 1, in which TO, Kr and CaL were each varied within 91 increments (91^3 = 753,571 permutations) were fitted to clinically measured MAP durations predicting VT/VF or mortality. C) Ionic pathway densities for dataset 2, in which 753,571 permutations of TO, Kr and CaL were fitted to measured MAP durations predicting VT/VF or mortality. *Action potentials from patients with VT/VF* exhibited lower Kr, higher CaL or enhanced NCX (explaining higher phase II plateau) than those without events. *Action potentials from patients who died* exhibited elevated Kr or reductions in NCX compared to those who survived.

Table 1.

Baseline Characteristics of Population Split by Endpoint of VT or VF at 3-years

	All Subjects (n=42)	VT/VF at 3 years (n=13)	No VT/VF at 3 years (n=29)	p
Age, y	64.7 ± 13.0	65.5 ± 12.4	64.3 ± 12.0	0.781
Gender, M/F	41/1	13/0	28/1	1
LVEF, %	27.0 ± 7.6	27.2 ± 8.1	26.9 ± 7.4	0.896
QRS Duration, ms	126 ± 33	128 ± 37	125 ± 32	0.766
LBBB, % (n)	28.6 (12)	23.1 (3)	31.0 (9)	0.725
RBBB, % (n)	14.3 (6)	23.1 (3)	10.3 (3)	0.341
IVCD, % (n)	21.4 (9)	53.8 (7)	6.9 (2)	0.697
Any IVCD, % (n)	64.3 (27)	61.5 (8)	65.5 (19)	1
Myocardial Infarct, % (n)	88.1 (37)	92.3 (12)	86.6 (25)	1
Days from MI to EPS (IQR)	3036 (1319-7015)	6681 (2627-7771)	2914 (943-6771)	0.205
Days from revasc. to EPS (IQR)	2495 (1260-4714)	2221 (292-4861)	2529 (1379-4714)	0.418
CAD Vessels, % (n)				
LAD	59.5 (25)	46.2 (6)	65.5 (19)	0.237
LCx	54.8 (23)	38.5 (5)	62.1 (18)	0.296
RCA	61.9 (26)	61.5 (8)	62.1 (18)	1
Hypertension, % (n)	19.0 (8)	23.1 (3)	17.2 (5)	0.686
Diabetes, % (n)	14.3 (6)	15.4 (2)	13.8 (4)	1
Laboratory values				
BNP, pg/ml (median, IQR)	341 (157–999)	389 (124–1120)	299 (162–908)	0.806
Sodium, mmol/L	139 ± 3.6	139 ± 3.5	138 ± 3.6	0.48
Potassium, mmol/L	4.3 ± 0.4	4.4 ± 0.3	4.4 ± 0.5	0.922
Magnesium, mmol/L	2.0 ± 0.4	2.1 ± 0.2	2.0 ± 0.4	0.142
Prior Medications, % (n)				
Beta-Blocker	73.8 (31)	69.2 (9)	75.9 (22)	0.713
ACE inhibitors/ARB	92.9 (39)	100 (13)	89.7 (26)	0.54
Spironolactone	19.0 (8)	30.8 (4)	13.8 (4)	0.226
CCB	14.3 (6)	7.7 (1)	17.2 (5)	0.647
Digoxin	38.1 (16)	30.8 (4)	41.4 (12)	0.733
Amiodarone	9.5 (4)	15.4 (2)	6.9 (2)	0.576
Statins	71.4 (30)	69.2 (9)	72.4 (21)	1
Implantable Device at EPS *	85.7 (36)	100.0 (13)	79.3 (23)	0.153

* within 14 days

Key: Values are n, mean ± standard deviation, or median (interquartile range). Categorical variables are compared using Fisher's exact test; continuous variables using the t-test (except BNP: Mann-Whitney U test performed because data is not normally distributed). ACE, angiotensin converting enzyme; ARB, angiotensin receptor blockers; BNP, B-type natriuretic peptide concentration; CCB, calcium channel blockers; CAD, coronary artery disease; EPS, electrophysiology study; IVCD, intraventricular conduction delay; LAD, left anterior descending artery; LBBB, left

bundle branch block; LCx, left circumflex artery; MI, myocardial infarction; RBBB, right bundle branch block; RCA, right coronary artery; Revasc., coronary revascularization; Statins, HMG-CoA reductase inhibitors.

Table 2.

Patient-level Decision Statistics of MAP Scores for Sustained VT/VF (%) and All-Cause Mortality (%)

	Sustained VT/VF			All-Cause Mortality		
		95% Confidence Limits			95% Confidence Limits	
	Percent	Lower	Upper	Percent	Lower	Upper
Sensitivity	84.6	54.6	98.1	85.7	57.2	98.2
Specificity	86.2	68.3	96.1	78.6	59	91.7
Positive Predictive Value (PPV)	73.3	44.9	92.2	66.7	41	86.7
Negative Predictive Value (NPV)	92.6	75.7	99.1	91.7	73	99
Accuracy	85.7	71.5	94.6	81	65.9	91.4

Table 3.

Univariate and Multivariate Predictors of Sustained VT/VF and Mortality

	Sustained VT/VF Endpoint			All-Cause Mortality Endpoint		
Predictor	**Univariate p**	**Multivariate p**	**OR (95% CI)**	**Univariate p-value**	**Multivariate p**	**OR (95% CI)**
Age (years)	0.695			0.011		
LVEF (%)	0.8			0.664		
Heart Rate (bpm)	0.45			0.622		
QRS Duration (ms)	0.759			0.486		
LBBB	0.651			0.507		
RBBB	0.246			0.246		
IVCD	0.563			0.385		
Any IVCD	0.941			0.871		
CAD Vessels						
LAD	0.285			0.542		
LCx	0.185			0.720		
RCA	0.885			0.750		
Time of Event to EPS						
Days from MI to EPS	0.199			0.076		
Days from revasc. To EPS	0.589			0.389		
HTN	0.321			0.307		
Diabetes	0.702			0.452		
Log 10 BNP (pg/mL)	0.829			0.012		
Prior Beta-blocker use	0.748			0.002	0.018	0.058 (0.006-0.618)
Prior CCB use	0.369			0.403		
Prior amiodarone use	0.431			0.507		
Prior ACEi/ARB use	0.211			0.232		
Prior digoxin use	0.542			0.123		
Prior spironolactone use	0.125			0.695		
Prior statin use	0.748			0.528		
Inducible Arrhythmias	0.750			0.445		
Implantable Device at EPS	0.999			0.999		
MAP Score Group	<0.001	<0.001	24.20 (4.03-145.30)	<0.001	0.003	31.0 (3.2-299.0)

Notes: ACEi, angiotensin converting enzyme inhibitor; ARB, angiotensin receptor blocker; BNP, B-type natriuretic peptide; CAD, coronary artery disease; CCB, calcium channel blocker; statin, HMG-CoA reductase inhibitors; HTN, hypertension; IVCD, intraventricular conduction delay; LAD, left anterior descending artery; LBBB, left bundle branch block; LCx, left circumflex artery; LVEF, left ventricular ejection fraction; MAP Score Group indicates patients above the ROC cut point for the MAP Score for VT/VF or mortality, respectively. RBBB, right bundle branch block; RCA, right coronary artery, Statins, QRS duration in milliseconds.